This is an Accepted Manuscript of an article published by Elsevier Biochemical Pharmacology

Final publication is available at
http://www.sciencedirect.com/science/article/pii/S0006295212001645

© 2014. This manuscript version is made available under the CC-BY-NC-ND 4.0 license http://creativecommons.org/licenses/by-nc-nd/4.0/

Characterisation of Na_v types endogenously expressed in human SH-SY5Y neuroblastoma cells

Irina Vetter[1], Christine A Mozar[2], Thomas Durek[1], Joshua S Wingerd[1], Paul F Alewood[1], Macdonald J Christie[2], Richard J Lewis[1]

[1]Institute for Molecular Bioscience, The University of Queensland, St Lucia, QLD 4072, Australia

[2]Brain & Mind Research Institute, The University of Sydney, NSW 2006, Australia

Running title: $Na_v1.7$ functional expression

All correspondence should be addressed to:

Richard J. Lewis, Institute for Molecular Bioscience, The University of Queensland, St Lucia QLD 4072, Australia, Tel: +61 7 334 62374, Fax: +61 7 334 62984, e-mail: r.lewis@imb.uq.edu.au

Abbreviations: Na_v, voltage-gated sodium channel; TTX, tetrodotoxin; ProTxII, β/ω-theraphotoxin-Tp2a; Ca^{2+}, calcium ion; DMEM, Dulbecco's Modified Eagle's Medium; FBS, foetal bovine serum; PBS, phosphate buffered saline; PSS, physiological salt solution; HBS, HEPES-buffered saline; AFU, arbitrary fluorescence unit; SEM, standard error of the mean; Fluo-4 AM, Fluo-4 acetoxymethylester; RPMI, Roswell Park Memorial Institute; BSA, bovine serum albumin; CCD, charge-coupled device; DAPI, 4',6-diamidino-2-phenylindole

Abstract

The human neuroblastoma cell line SH-SY5Y is a potentially useful model for the identification and characterisation of Na_v modulators, but little is known about the pharmacology of their endogenously expressed Na_vs. The aim of this study was to determine the expression of endogenous Na_v α and β subunits in SH-SY5Y cells using PCR and immunohistochemical approaches, and pharmacologically characterise the Na_v isoforms endogenously expressed in this cell line using electrophysiological and fluorescence approaches. SH-SY5Y human neuroblastoma cells were found to endogenously express several Na_v isoforms including $Na_v1.2$ and $Na_v1.7$. Activation of endogenously expressed Na_vs with veratridine or the scorpion toxin OD1 caused membrane depolarization and subsequent Ca^{2+} influx through voltage-gated L- and N-type calcium channels, allowing Na_v activation to be detected with membrane potential and fluorescent Ca^2 dyes. μ-Conotoxin TIIIA and ProTxII identified $Na_v1.2$ and $Na_v1.7$ as the major contributors of this response. The $Na_v1.7$-selective scorpion toxin OD1 in combination with veratridine produced a $Na_v1.7$-selective response, confirming that endogenously expressed human $Na_v1.7$ in SH-SY5Y cells is functional and can be synergistically activated, providing a new assay format for ligand screening.

Key Words: SH-SY5Y; Ca^{2+}; $Na_v1.7$; ProTxII; OD1

1. Introduction

Voltage-gated sodium channels (Na_v) are complex transmembrane proteins comprised of a pore-forming α subunit and accessory β subunits that play an essential role in the initiation and propagation of action potentials in excitable cells. To date, apart from the related Na_x which appears to function as a sodium sensor [1, 2], nine isoforms termed $Na_v1.1$ – $Na_v1.9$ have been functionally defined as sodium-selective ion channels [3]. Their distinct tissue distribution and amenability to modulation by toxins and drugs has led to significant interest in Na_v as therapeutic targets in a number of poorly treated conditions ranging from epilepsy to cardiac arrhythmias and pain [4]. In recent years $Na_v1.7$ has emerged as an attractive drug target, with expression restricted to a subset of nociceptive neurons that is expected to limit on-target side effects of pharmacological modulators of $Na_v1.7$ [5]. In addition, loss-of-function mutations in humans have highlighted the possibility that $Na_v1.7$ inhibition could produce complete loss of pain sensations without dose-limiting side effects [6]. However, it remains unclear if such an effect can be translated to the clinic given the lack of subtype-specific $Na_v1.7$ blockers in clinical trials.

Neuroblastoma and other cell lines of neuronal origin have been widely used for the identification and characterisation of putative and clinically used therapeutics with activity at Na_v. In this context, cell lines of human origin, such as SH-SY5Y human neuroblastoma cells, are particularly useful as they endogenously express human targets in cell types of neuronal origin. However, knowledge of the endogenous Na_v α and β subtype expression in these neuronal cell lines is incomplete, limiting the interpretation of pharmacological data obtained from these cell lines. Using PCR, immunohistochemistry, electrophysiology and fluorescence-based responses, we have characterised the Na_v types expressed in human SH-SY5Y

neuroblastoma cells and used toxins to establish assays that can detect modulators of human $Na_v1.2$ and/or $Na_v1.7$.

2. Methods

2.1 Materials

Veratridine was obtained from Ascent Scientific (Bristol, UK), tetrodotoxin (TTX) was from Enzo Life Sciences (Farmingdale, NY, USA) and ProTxII and Agatoxin TK were from Peptides International (Lousiville, KY, USA). Synthetic CVID, TIIIA, GIIIA were obtained through total synthesis as described previously [7-9]. Scorpion toxin OD1 was prepared by a combination of solid-phase peptide synthesis and chemical ligation [10]. All other reagents, unless otherwise stated, were obtained from Sigma Aldrich (Castle Hill, NSW, Australia). TTX, veratridine, ProTxII, OD1 and TIIIA were routinely diluted in 0.3–0.5 % bovine serum albumin (BSA) solution to avoid adsorption to plastic surfaces.

2.2 Cell Culture

SH-SY5Y human neuroblastoma cells were a kind gift from Victor Diaz (Max Planck Institute for Experimental Medicine, Goettingen, Germany). Cells were routinely maintained in RPMI medium (Invitrogen, Australia) supplemented with 15 % foetal bovine serum and L-glutamine and passaged every 3–5 days using 0.25 % trypsin/EDTA (Invitrogen). Cells were plated at a density of 120, 000–150, 000 cells/well on 96-well or 30, 000–50, 000 cells/well on 384-well black-walled imaging plates (Corning) 48 h prior to FLIPR assays. For electrophysiological studies, SH-SY5Y cells were maintained in Dulbecco's Modified Eagle's Medium (DMEM)

containing 4.5 g/L D-glucose, 0.584 g/L L-Glutamine and 110 mg/L sodium pyruvate (Invitrogen). DMEM was supplemented with 10 % heat inactivated foetal bovine serum, 1 % Penicillin and Streptomycin (10, 000 units/ml and 10, 000 μg/ml, respectively; Invitrogen). Cells were passaged every 4–5 days with 0.25 % trypsin (Invitrogen) and plated at low density in 35 x 10 mm culture dishes (BD Corning, North Ryde, NSW, Australia) at least 24 hours prior to electrophysiological recordings. Robust Na_v responses were observed over a period of approximately 3 years and up to 20 passages.

2.3 Whole-cell patch-clamp electrophysiology

SH-SY5Y cells were used within 24–72 hours of plating. Only cells with minimal or no processes were used. Whole-cell patch-clamp recordings were performed at room temperature with fire-polished patch electrodes prepared from borosilicate glass (SDR Clinical Technology, Middle Cove, NSW, Australia). Electrode resistance was 3.5–5 MΩ when filled with an internal solution containing (composition in mM): 120 CsCl, 5 MgATP, 5 NaCl, 2 $CaCl_2$, 20 HEPES, 10 EGTA, pH 7.3 and adjusted to 283-286 mOsm. Cells were continuously bathed in a HEPES-buffered physiological saline (HBS; composition in mM): 155 NaCl, 2.5 KCl, 1.8 $CaCl_2$, 1.2 $MgCl_2$, 10 HEPES, 10 glucose, pH 7.4 (adjusted with NaOH) and adjusted to 328-331 mOsm. Recordings were made with a HEKA EPC-9 amplifier and PULSE software (v 8.8, HEKA Elektronik, Lambrecht/Pfalz, Germany). Data was filtered at 4 kHz and sampled at 20 kHz. Mean cell capacitance was 4.96 pF and series resistance was 5.9 MΩ, which was compensated by 80%. Capacitance transients were compensated and leak subtraction was performed with a *P*/8 protocol except during experiments using veratridine (to avoid subtraction of any

veratridine-induced steady state currents). Drugs were applied to cells by superfusion through gravity-fed flow pipes (250 µm diameter) positioned directly above the cell.

2.4 Fluorescence measurement of membrane potential changes

To assess changes in membrane potential, SH-SY5Y cells were loaded with the red membrane potential dye (Molecular Devices, Sunnyvale, CA) according to the manufacturer's instructions. In brief, red membrane potential dye (proprietary composition) was reconstituted with a volume of physiological salt solution (PSS; composition in mM: NaCl 140, glucose 11.5, KCl 5.9, $MgCl_2$ 1.4, NaH_2PO_4 1.2, $NaHCO_3$ 5, $CaCl_2$ 1.8, HEPES 10) as specified in the manufacturer's instructions and after a wash with PSS, cells were incubated with 100 µl of the membrane potential solution at 37 ˚C for 30 min. The cells were then transferred to the FLIPR^{TETRA+} fluorescent plate reader and changes in fluorescence (excitation 510–545 nm; emission 565–625 nm) in response to addition of agonists was measured every second for 300 s.

2.5 Fluorescence measurement of calcium responses

SH-SY5Y cells were loaded with the fluorescent calcium dye Fluo-4 by incubating the cells in PSS containing 0.3 % bovine serum albumin and 4 µM Fluo-4-AM (Invitrogen) for 30 min at 37 ˚C. To remove extracellular dye and facilitate dye hydrolysis, cells were washed with PSS for 5–15 min prior to loading of plates into the FLIPR^{TETRA+} (Molecular Devices, Sunnyvale, CA) fluorescent plate reader. Fluorescence (excitation 470–495 nm; emission 515–575 nm) was measured using a cooled charge-coupled device (CCD) camera with camera gain and excitation intensity adjusted for each plate to yield an average baseline fluorescence value of 1000 AFU.

After 10 baseline reads, buffer or antagonists were added and the fluorescence response was measured every second for 300 reads, followed by addition of agonists and fluorescence measurements every second for a further 300 seconds. For ProTxII, an additional read interval of 150 reads every 10 s was incorporated prior to addition of agonists to extend the total incubation time to 30 min. Raw fluorescence readings were converted to response over baseline using the analysis tool of Screenworks 3.1.1.4 (Molecular Devices) and were expressed relative to the maximum increase in fluorescence of control responses.

2.6 Immunofluorescence

SH-SY5Y cells were plated on PDL-coated glass coverslips at a density of 1 x 10^5 cells/well in 12 well plates and grown for 48–72 h. After a wash with PBS (phosphate buffered saline; Invitrogen) cells were fixed for 30 min at room temperature with Histochoice® MB fixative (Solon, OH, USA), permeabilised for 10 min with 0.1 % Triton-X 100 and blocked with 3 % BSA for 30 min at room temperature. After a 1 h incubation with rabbit anti-$Na_v1.7$ primary antibody (Alomone Labs, Jerusalem), cells were washed several times with PBS and stained with anti-rabbit Alexa-488 (Invitrogen) and DAPI to visualize nuclei. Cells were imaged with a Zeiss Axiovert 200 Inverted Laser Scanning Confocal microscope using a Plan Apochromat 100 x/1.4 oil immersion lens.

2.7 Semi-quantitative PCR

SH-SY5Y cells were grown on 10 cm dishes, washed twice with ice-cold PBS and total RNA isolated using the Qiagen RNeasy Plus Mini Kit (Qiagen) according to the manufacturer's

instructions with on-column DNA digestion. The Omniscript Reverse Transcription Kit (Qiagen) was used to reverse transcribe 1 μg of RNA, as determined by spectrophotometric absorbance at 260 nm, and 20 ng of the resulting cDNA was amplified using the Platinum® Pfx kit (Invitrogen). PCR reactions additionally contained final concentrations of 2 x amplification buffer, 0.3 mM dNTP, 1 mM $MgCl_2$, 0.4 μM primers and 1 U Pfx polymerase in a volume of 50 μl and were amplified under the following conditions: 94 °C for 5 min, 30 cycles of 94 for 15 s, 60-64 for 30 s, 68 for 1 min and a final extension at 68 for 10 min. Human Na_v primers were designed using Primer BLAST, and human β subunit primers were as previously described in the literature [11] (see Table 1). Plasmids encoding for $Na_v1.1$–1.8 and β1–β3 subunits verified amplification of the correct products for each subtype (data not shown). All reaction products were analysed on 2% agarose gels and band density was determined using BioRad Quantity One V4.5.2 build 70 with background correction.

2.7 Z' factor determination of assay robustness

The Z' factor, a quantitative representation of assay quality, was determined as previously described [12], with 48 replicates of a negative control (PSS) and 48 replicates of positive controls (50 μM veratridine or 30 nM OD1 + 2 μM veratridine) per plate. Mean and standard deviation for positive and negative controls were determined using GraphPad Prism (Version 4.00, San Diego, California) and the Z' factor for each plate determined according to the following equation:

$$Z' = 1 - ((3SD_{positive} + 3SD_{negative})/(mean_{positive} - mean_{negative}))$$

2.8 Data analysis

Unless otherwise stated, all data are expressed as the mean ± standard error of the mean (SEM) determined from at least n = 3 replicates and are representative of at least 2–4 independent experiments. To establish concentration-response curves, responses after addition of compounds were plotted against agonist concentration and a 4-parameter Hill equation with variable Hill slope or a two-site model was fitted to the data using GraphPad Prism (Version 4.00, San Diego, California). Potency of agonists and antagonists are reported as the mean ± SEM of 3–4 separate experiments. Electrophysiological data were analysed with Pulsefit (v 8.8, HEKA Electronics) and GraphPad Prism (v 4.0b for Macintosh, GraphPad Software Inc., San Diego, California, USA) software. AxographX (Axograph Scientific, Australia) was used to generate all electrophysiological images for figures presented. Statistical significance was determined using an unpaired student's *t*-test with statistical significance defined as $p < 0.05$ unless otherwise stated.

3. Results

3.1 SH-SY5Y cells endogenously express TTX-sensitive Na_v channels

We assessed expression of human TTX-sensitive and TTX-resistant Na_v isoforms and the accessory β subunits present in SH-SY5Y cells by semi-quantitative PCR. As previously reported, SH-SY5Y cells expressed mainly the TTX-sensitive isoforms $Na_v1.3$ and $Na_v1.7$ as well as $Na_v1.2$ (Fig 1 A) [13]. In addition, we also detected some amplification of $Na_v1.4$ and $Na_v1.5$. In contrast to previous reports we were unable to detect $Na_v1.9$ [13], while $Na_v1.7$ was consistently the most highly expressed Na_v isoform in SH-SY5Y cells. In addition, we did not

detect $Na_v1.7$ transcripts in the commonly used rat neuronal cell line PC12 or NG108-15 mouse neuroblastoma X rat glioma hybrid cells (data not shown). In SH-SY5Y cells, β2 and β3 but not β1 or β4 subunits were also amplified (Fig 1 B). We confirmed $Na_v1.7$ protein trafficked correctly to the plasma membrane by immunofluorescence (Fig 2 A and B). SH-SY5Y cells stained with a $Na_v1.7$ antibody showed fluorescence localized to the plasma membrane (Fig 2 A and B), consistent with functional Na_v expression.

3.2 Endogenously expressed TTX-sensitive Na_v in SH-SY5Y cells are functional and activated by veratridine

To establish that Na_v isoforms expressed in SH-SY5Y cells are functional, we assessed voltage-gated sodium currents in SH-SY5Y cells using whole-cell patch clamp recording. As previously reported [14, 15], depolarizing pulses elicited TTX-sensitive I_{Na} in undifferentiated SH-SY5Y cells (Fig 3 A). The I_{Na}, evoked by stepping from –90 mV to 0 mV for 10 ms was blocked by TTX in a concentration-dependent manner, with minimal inhibition at 1 nM and marked inhibition from 30–300 nM (Fig 3 B and C; pIC_{50} 8.3 ± 0.08). Inhibition by TTX was largely reversible, as seen by the washout in the time plot in Fig 3 B.

As the sodium channel activator veratridine is commonly used to elicit Na_v responses in high-throughput assays where control over membrane potential is not possible, we also assessed the effect of veratridine on I_{Na} in SH-SY5Y cells. Veratridine (50 μM) was superfused onto SH-SY5Y cells and a veratridine-induced, sustained tail current evoked by 10 ms depolarization steps from –90 mV to 0 mV every 2.5 s (i.e. 5 depolarization steps) at 30 s intervals. Repetitive

stimulation of Na_v by high frequency depolarization keeps Na_v in the open state, permitting maximal veratridine binding, and production of a sustained Na_v tail current at resting membrane potential [16]. This veratridine-induced effect was mediated by TTX-sensitive Na_v, as superfusion of TTX (1 μM) completely abolished veratridine-induced tail currents (Fig 3 D).

Modulation of endogenously expressed Na_v isoforms in SH-SY5Y cells by veratridine also resulted in membrane potential changes measured using the "red" FLIPR membrane potential dye. Addition of veratridine caused concentration-dependent membrane depolarization with an EC_{50} of 28.5 μM (pIC_{50} 4.54 ± 0.06; Fig 3 E) confirming that Na_v channels endogenously expressed in SH-SY5Y cells are indeed functional and can be activated by veratridine (Fig 3 F). The veratridine-induced membrane depolarization was mediated only through activation of TTX-sensitive Na_v, as pre-treatment with TTX (300 nM) completely abolished these responses (Fig 3 E and F).

In rat cortical synaptosomes and CA1 hippocampal pyramidal neurons, activation of Na_v by veratridine leads to cell depolarization and downstream influx of Ca^{2+} [17, 18]. We wanted to assess if veratridine-induced Ca^{2+} influx also occurs in SH-SY5Y cells, and which ion channels contribute to this response. Detection of veratridine-induced responses based on fluorescent calcium (Ca^{2+}) signalling would also be suitable as a robust and cost-effective Na_v assay that avoids some of the weaknesses of membrane potential assays which are prone to artefacts and costly. Indeed, addition of veratridine caused a concentration-dependent increase in intracellular calcium with an EC_{50} of 12.7 μM (pIC_{50} 4.89 ± 0.11; Fig 4 A). The Hill slope of the veratridine-induced response was surprisingly steep (3.25 ± 0.9 in the membrane potential assay and 4.2 ±

0.6 in the Ca^{2+} response assay), with small changes in veratridine concentration eliciting large increases in fluorescence emission. The Ca^{2+} responses elicited by veratridine were completely abolished in the presence of TTX (300 nM), confirming these responses were mediated solely through TTX-sensitive Na_v isoforms endogenously expressed in SH-SY5Y cells (Fig 4 A and B). The IC_{50} of TTX-mediated inhibition of veratridine responses was 8.6 nM (pIC_{50} 8.06 ±0.08) (Fig 4 B), consistent with the inhibition of TTX-sensitive Na_v channels, and best fitted by a single site fit.

3.3 L-type and N-type calcium channels contribute to the veratridine-induced response

To assess which voltage-gated calcium channels contribute to the depolarization-induced Ca^{2+} influx after addition of veratridine, we assessed the effects of nifedipine to block L-type voltage-gated calcium channels (VGCC) [19], ω-conotoxin CVID to block N-type VGCC [7], and ω-agatoxin TK to block P/Q-type VGCC [20], on the veratridine-induced responses (Fig 4 C and D). Pre-treatment with nifedipine concentration-dependently inhibited veratridine-induced responses with an IC_{50} of 10.7 nM (pIC_{50} 7.97 ± 0.2) (Fig 4 C). However, nifedipine did not completely abolish veratridine-induced responses, with 23.9 ± 4.4 % of the response remaining in the presence of saturating concentrations of nifedipine. The veratridine-induced response was also mediated by N-type VGCC, as CVID also caused a partial (31.8 ± 1.1%) concentration-dependent block (pIC_{50} 7.7 ± 0.5) of the veratridine-induced response (Fig 4 D). In contrast, the $Ca_v2.1$ antagonist agatoxin TK did not inhibit veratridine responses (Fig 4 C). Co-addition of nifedipine (10 µM) and CVID (1 µM) completely abolished veratridine-mediated responses (Fig 4 D), confirming only $Ca_v2.2$ and nifedipine-sensitive L-type calcium channels were involved.

3.4 Na_v subtypes contributing to the veratridine-induced response

We used Na_v subtype-specific inhibitors to elucidate the contribution of various Na_v subtypes to the veratridine-induced Ca^{2+} response. Although $Na_v1.2$ was not the most abundantly expressed Na_v isoform in SH-SY5Y cells as determined by RT-PCR, the $Na_v1.2/1.4$-selective blocker TIIIA [8] reduced veratridine-induced responses by 42.6 ± 6.8 % (Fig 4 E; n= 4 independent experiments) with an IC_{50} of 290 nM (pIC_{50} 6.54 ± 0.09). This component was mediated exclusively by $Na_v1.2$, as the $Na_v1.4$-selective blocker GIIIA [21] failed to inhibit veratridine responses (Fig 4 E) at concentrations up to 10 µM. A small but significant ($p < 0.05$) rightward shift of the veratridine concentration-response curve was observed in the presence of TIIIA (1 µM) (veratridine EC_{50} 45.8 µM; pEC_{50} 4.33 ± 0.16) and TIIIA again decreased the magnitude of the response by 41.3 ± 2.8% (Fig 4 F).

The component of the veratridine-induced response observed in the presence of TIIIA was completely blocked by the $Na_v1.7$-selective blocker ProTxII [22] (IC_{50} of 206.9 pM; pIC_{50} 9.68 ± 0.15, n = 4 independent experiments) consistent with inhibition of $Na_v1.7$ (Fig 4 G). In the absence of TIIIA, ProTxII blocked veratridine-induced responses with a two-site fit with IC_{50}s of 151.7 pM and 56 nM (pIC_{50} 9.82 ± 0.23 and pIC_{50} 7.25 ± 0.26), consistent with high affinity inhibition of $Na_v1.7$ and lower affinity inhibition of $Na_v1.2$ and/or $Na_v1.3$ (Fig 4 G). This response displayed excellent robustness and reproducibility, with a Z' factor [12] of 0.7 ± 0.05 (Fig 4 H) and can be adapted into an assay format that can detect endogenously expressed human $Na_v1.2$ or $Na_v1.7$ either together or specifically in the presence of appropriate inhibitors.

Inhibition of endogenous Na_v currents in SH-SY5Y cells by ProTxII and TIIIA was further verified by electrophysiology techniques (Fig 5). Cultured SH-SY5Y cell I_{Na} was evoked by stepping from –90 mV to 0 mV for 10 ms. As summarized in Fig 5 A-C, ProTxII (30 nM) inhibited I_{Na} by 41 ± 1.9 % (n = 8; $p < 0.0001$, one-sample *t* test), and TIIIA (1 μM) inhibited I_{Na} by 31 ± 2.1 % (n = 6; $p < 0.0001$, one-sample t test). Co-application revealed an additive effect, with 64 % inhibition (n = 2) of I_{Na} in the presence of both ProTxII and TIIIA (Figure 5 A-C), with the residual TTXs component likely representing current mediated through $Na_v1.3$. In contrast, veratridine-evoked Ca^{2+} responses measured using the FLIPR were completely abolished in the presence of both ProTxII and TIIIA (Fig 4 G).

During repetitive Na_v activation, veratridine produces a slowly decaying Na_v tail current at resting membrane potentials [16, 18]. The veratridine-induced, sustained tail current at -90mV was partially inhibited by ProTxII (30 nM) and TIIIA (1 μM) also (Fig 5 D). In the presence of veratridine (50 μM), ProTxII (30 nM) inhibited the tail current by 55 ± 7.8 % (n = 13; $p < 0.0001$, one-sample *t* test) and TIIIA (1 μM) inhibition was 48 ± 7.7% (n = 6; $p = 0.0016$, one-sample *t* test). When both ProTxII (30 nM) and TIIIA (1 μM) were superfused onto cells in the presence of veratridine (50 μM), 77 ± 13% inhibition was observed (n = 4; $p = 0.009$, one-sample *t* test). TTX (1 μM) completely abolished the tail current (n = 3, data not shown).

These data reveal that $Na_v1.7$ contributes a substantial component to the I_{Na} and veratridine-induced Ca^{2+} responses in SH-SY5Y cells. To directly isolate the $Na_v1.7$ component from SH-SY5Y cells we investigated if the scorpion toxin OD1, a $Na_v1.7$-selective sodium channel

modulator from the Iranian scorpion *Odonthobuthus doriae* [10, 23], could activate Na_v endogenously expressed in SH-SY5Y cells. Exposure to OD1 caused a concentration-dependent leftward shift in the veratridine-induced Ca^{2+} concentration-response curve and markedly potentiated sub-threshold veratridine-induced Ca^{2+} responses (pEC_{50} 8.52 ± 0.02), while maximal veratridine-induced responses were not further potentiated (Fig 6 A and B). At veratridine concentrations which did not elicit responses in the absence of OD1 (2 μM), the OD1-potentiated Ca^{2+} responses were concentration-dependently inhibited by the $Na_v1.7$ inhibitor ProTxII (pIC_{50} 8.75 ± 0.13; Fig 6 C), while the $Na_v1.2/1.4$ inhibitor TIIIA had no significant effect (data not shown). This response was also amenable to the characterisation of small molecule Na_v inhibitors used clinically, including trifluoperazine (IC_{50} 3.2 μM), amitriptyline (IC_{50} 548 nM), lignocaine (IC_{50} 20.9 μM), carbamazepine (IC_{50} 64.8 μM), tetracaine (IC_{50} 447 nM), mexiletine (IC_{50} 12.9 μM) and lamorigine (IC_{50} 819 nM) (Fig. 7).

4. Discussion

Cell lines of neuronal origin, including SH-SY5Y human neuroblastoma cells, endogenously express Na_v with characteristics resembling native Na^+ currents. While these cell lines have been used routinely for the identification and characterisation of Na_v modulators, little is known about the identity and pharmacology of the endogenously expressed Na_v subtypes involved. In these cells, the alkaloid veratridine activated endogenously expressed $Na_v1.2$ and $Na_v1.7$ identified by PCR and immunohistochemistry, producing an influx of Na^+ ions and subsequent membrane depolarization. This membrane depolarization in turn leads to a Ca^{2+} influx through endogenously expressed voltage-gated L- and N-type calcium channels that can be detected by fluorescent Ca^{2+} dyes such as Fluo-4. The Na_v subtypes underlying the veratridine response were determined using subtype specific venom peptides, allowing establishment of specific assays for $Na_v1.7$ and $Na_v1.2$.

Using PCR, we confirmed that $Na_v1.2$, 1.3 and 1.7 but not $Na_v1.9$ are expressed in SH-SY5Y cells [13]. Consistent with a lack of TTX-resistant Na_v isoforms, both Ca^{2+} and membrane potential responses elicited by veratridine were completely abolished by low concentrations of TTX. In electrophysiological experiments, we observed inhibition of Na_v currents in single SH-SY5Y cells by TTX with an average IC_{50} of 4.9 nM (Fig 3 C), confirming functional expression of only TTX-sensitive Na_v isoforms. However, there was notable heterogeneity in the IC_{50} of TTX observed in individual cells, reflected in an average Hill slope of – 0.6. This heterogeneity of TTX potency in the voltage clamp studies likely reflects a spread of expression levels of different TTX-sensitive Na_v subtypes in SH-SY5Y cells, as $Na_v1.3$ and $Na_v1.2$ are inhibited by

TTX with IC_{50}s of 4 [24] and 12 nM [25], respectively, while human $Na_v1.7$ is inhibited at slightly higher TTX concentrations with an IC_{50} of 24 nM [26, 27].

Although we detected low levels of $Na_v1.4$ mRNA transcript, veratridine has been reported to block rather than activate the skeletal muscle Na_v isoforms $Na_v1.4$ [28]. Confirming the lack of involvement of this muscle subtype in veratridine-induced responses, the $Na_v1.4$ inhibitor GIIIA failed to inhibit any significant component of the veratridine-elicited Ca^{2+} responses. However, we were able to confirm for the first time the expression of $Na_v1.7$ in SH-SY5Y cells at the protein level, with $Na_v1.7$ immunofluorescence localized predominantly at the plasma membrane. This endogenous expression of human $Na_v1.7$ together with functionally relevant β2 and β3 subunits makes SH-SY5Y cells well suited to the study of native human $Na_v1.7$ pharmacology. Consistent with the patterns of expression, low concentrations of ProTxII inhibited ~ 50% of the response detected by FLIPR Ca^{2+} measurements and patch clamping, with inhibition by TIIIA confirming that most of the remaining component arose from activation of $Na_v1.2$ by veratridine.

Pharmacological characterisation of the veratridine-induced responses in SH-SY5Y cells shows that despite the relatively high expression of $Na_v1.3$, this isoform does not appear to contribute significantly to the veratridine-induced Ca^{2+} responses. While veratridine has been reported to affect gating of most Na_v isoforms, albeit with reduced efficacy at $Na_v1.8$ [29], by binding to site 2 in the S6 segment of the voltage sensor, the relative sensitivity and efficacy of veratridine across Na_v isoforms has not been established [30]. In addition, veratridine has been reported to be a partial agonist in foetal mouse brain cells and rat heart cells [31, 32]. Thus, differences in

the sensitivity or efficacy of activation of Na_v subtypes by veratridine might contribute to preferential activation of endogenously expressed $Na_v1.2$ and $Na_v1.7$ in SH-SY5Y cells. It is also unclear if expression of accessory subunits alters activation of Na_v isoforms by veratridine. Specifically, the altered inactivation kinetics of $Na_v1.3$ in the presence of β3 subunits [33] might contribute to the absence of $Na_v1.3$-mediated responses to veratridine. While compounds affecting function of VGCC can produce false positives in this system, such artefacts can also provide valuable information on putative off-target effects of the test compounds. For example, compounds that cause an increase in intracellular Ca^{2+} upon addition are likely to possess undesirable off-target effects and can be excluded immediately from further study. The effect of such compounds on VGCC can be easily verified using a K^+ depolarization assay and fluorescent Ca^{2+} imaging in SH-SY5Y cells.

Some studies have reported an inability to detect modulation of heterologously expressed $Na_v1.7$ by gating modifiers such as ProTxI using membrane potential dyes [34]. However, we were able to detect inhibition by pore blockers such as tetrodotoxin, μ-conotoxin TIIIA and clinically used compounds including amitriptyline and tetracaine (Fig 7), as well as inhibition by the state dependent blocker ProTxII through the measurement of Ca^{2+} fluxes. This discrepancy may reflect expression of endogenous sodium channels in SH-SY5Y cells at a more physiological membrane potential compared to commonly used over-expression systems such as HEK293 cells [35, 36]. In addition, the human Na_v in SH-SY5Y cells are co-expressed with functionally relevant β-subunits, which could affect inhibition of Na_v activity by state-dependent blockers such as ProTxII. Thus, this assay is amenable to the measurement of a diverse range of modulators of Na_v function via detection of changes in Ca^{2+} signalling. Using the industry-

standard FLIPR platform in 96- or 384-well format we achieved a high signal-to-noise ratio (Z' score of 0.7), making this assay suitable for rapid identification of novel Na_v blockers.

As an alternative approach to generating $Na_v1.7$ specific responses, we investigated the potential of the scorpion toxin OD1, which affects inactivation of $Na_v1.7$ with high specificity [23], to synergise with veratridine. Treatment with OD1 caused a marked shift in the veratridine concentration-response curve producing responses that are now fully blocked by ProTxII. This demonstrates that the delay in $Na_v1.7$ inactivation induced by OD1, in combination with a shift in the voltage-dependence of Na_v activation elicited by veratridine, generates Ca^{2+} influx that is mediated solely through $Na_v1.7$. These results confirm the preferential activation of endogenous $Na_v1.7$ over $Na_v1.2$ by OD1 [10, 23] and permit assessment of human $Na_v1.7$ responses in an endogenous context without the need for addition of antagonists. At high concentrations, OD1 also effects a hyperpolarizing shift in the voltage of activation of $Na_v1.7$ [23], which presumably forms the basis for the small Ca^{2+} transients elicited by OD1 at high (> 30 nM) but not lower concentrations (data not shown). In contrast, at low concentrations OD1 affects the gating of $Na_v1.7$ and specifically impairs fast inactivation [10, 23], so that small shifts in the voltage-dependence of activation induced by veratridine result in synergistic activation of $Na_v1.7$. This allosteric interaction of veratridine with OD1 is consistent with their activity at site 3 and 2, respectively.

In conclusion, we have characterised Na_v endogenously expressed in the human neuroblastoma cell line SH-SY5Y and described assays which are able to detect activity of endogenously expressed human $Na_v1.2$ and/or $Na_v1.7$. Using this approach, both pore blockers and gating

modifiers of human sodium channels could be detected using fluorescence, providing a flexible, low cost alternative for the primary identification of novel Na_v modulators.

Acknowledgements: This work was supported by a NHMRC Australian Based Biomedical Postdoctoral Fellowship (IV), an NHMRC Biomedical Postgraduate Scholarship No. 571240 (CAM), NHMRC Professorial Research Fellowships (RJL and MJC), and an NHMRC Program Grant (RJL, PFA and MJC).

References

[1] Shimizu H, Watanabe E, Hiyama TY, Nagakura A, Fujikawa A, Okado H, et al. Glial Nax channels control lactate signaling to neurons for brain [Na+] sensing. Neuron 2007;54:59-72.

[2] Hiyama TY, Watanabe E, Ono K, Inenaga K, Tamkun MM, Yoshida S, et al. Na(x) channel involved in CNS sodium-level sensing. Nat Neurosci 2002;5:511-2.

[3] Yu FH, Catterall WA. Overview of the voltage-gated sodium channel family. Genome Biol 2003;4:207.

[4] Clare JJ, Tate SN, Nobbs M, Romanos MA. Voltage-gated sodium channels as therapeutic targets. Drug Discov Today 2000;5:506-20.

[5] Dib-Hajj SD, Cummins TR, Black JA, Waxman SG. Sodium channels in normal and pathological pain. Annu Rev Neurosci 33:325-47.

[6] Cox JJ, Reimann F, Nicholas AK, Thornton G, Roberts E, Springell K, et al. An SCN9A channelopathy causes congenital inability to experience pain. Nature 2006;444:894-8.

[7] Lewis RJ, Nielsen KJ, Craik DJ, Loughnan ML, Adams DA, Sharpe IA, et al. Novel omega-conotoxins from Conus catus discriminate among neuronal calcium channel subtypes. J Biol Chem 2000;275:35335-44.

[8] Lewis RJ, Schroeder CI, Ekberg J, Nielsen KJ, Loughnan M, Thomas L, et al. Isolation and structure-activity of mu-conotoxin TIIIA, a potent inhibitor of tetrodotoxin-sensitive voltage-gated sodium channels. Mol Pharmacol 2007;71:676-85.

[9] Nielsen KJ, Watson M, Adams DJ, Hammarstrom AK, Gage PW, Hill JM, et al. Solution structure of mu-conotoxin PIIIA, a preferential inhibitor of persistent tetrodotoxin-sensitive sodium channels. J Biol Chem 2002;277:27247-55.

[10] Jalali A, Bosmans F, Amininasab M, Clynen E, Cuypers E, Zaremirakabadi A, et al. OD1, the first toxin isolated from the venom of the scorpion Odonthobuthus doriae active on voltage-gated Na+ channels. FEBS Lett 2005;579:4181-6.

[11] Diss JK, Fraser SP, Walker MM, Patel A, Latchman DS, Djamgoz MB. Beta-subunits of voltage-gated sodium channels in human prostate cancer: quantitative in vitro and in vivo analyses of mRNA expression. Prostate Cancer Prostatic Dis 2008;11:325-33.

[12] Zhang JH, Chung TD, Oldenburg KR. A Simple Statistical Parameter for Use in Evaluation and Validation of High Throughput Screening Assays. J Biomol Screen 1999;4:67-73.

[13] Blum R, Kafitz KW, Konnerth A. Neurotrophin-evoked depolarization requires the sodium channel Na(V)1.9. Nature 2002;419:687-93.

[14] Brown NA, Kemp JA, Seabrook GR. Block of human voltage-sensitive Na+ currents in differentiated SH-SY5Y cells by lifarizine. Br J Pharmacol 1994;113:600-6.

[15] Toselli M, Tosetti P, Taglietti V. Functional changes in sodium conductances in the human neuroblastoma cell line SH-SY5Y during in vitro differentiation. J Neurophysiol 1996;76:3920-7.

[16] Sutro JB. Kinetics of veratridine action on Na channels of skeletal muscle. J Gen Physiol 1986;87:1-24.

[17] Meder W, Fink K, Gothert M. Involvement of different calcium channels in K+- and veratridine-induced increases of cytosolic calcium concentration in rat cerebral cortical synaptosomes. Naunyn Schmiedebergs Arch Pharmacol 1997;356:797-805.

[18] Fekete A, Franklin L, Ikemoto T, Rozsa B, Lendvai B, Sylvester Vizi E, et al. Mechanism of the persistent sodium current activator veratridine-evoked Ca elevation: implication for epilepsy. J Neurochem 2009;111:745-56.

[19] Catterall WA, Perez-Reyes E, Snutch TP, Striessnig J. International Union of Pharmacology. XLVIII. Nomenclature and structure-function relationships of voltage-gated calcium channels. Pharmacol Rev 2005;57:411-25.

[20] Teramoto T, Kuwada M, Niidome T, Sawada K, Nishizawa Y, Katayama K. A novel peptide from funnel web spider venom, omega-Aga-TK, selectively blocks, P-type calcium channels. Biochem Biophys Res Commun 1993;196:134-40.

[21] Lopez-Vera E, Walewska A, Skalicky JJ, Olivera BM, Bulaj G. Role of hydroxyprolines in the in vitro oxidative folding and biological activity of conotoxins. Biochemistry 2008;47:1741-51.

[22] Schmalhofer WA, Calhoun J, Burrows R, Bailey T, Kohler MG, Weinglass AB, et al. ProTx-II, a selective inhibitor of NaV1.7 sodium channels, blocks action potential propagation in nociceptors. Mol Pharmacol 2008;74:1476-84.

[23] Maertens C, Cuypers E, Amininasab M, Jalali A, Vatanpour H, Tytgat J. Potent modulation of the voltage-gated sodium channel Nav1.7 by OD1, a toxin from the scorpion Odonthobuthus doriae. Mol Pharmacol 2006;70:405-14.

[24] Meadows LS, Chen YH, Powell AJ, Clare JJ, Ragsdale DS. Functional modulation of human brain Nav1.3 sodium channels, expressed in mammalian cells, by auxiliary beta 1, beta 2 and beta 3 subunits. Neuroscience 2002;114:745-53.

[25] Westenbroek RE, Merrick DK, Catterall WA. Differential subcellular localization of the RI and RII Na+ channel subtypes in central neurons. Neuron 1989;3:695-704.

[26] Klugbauer N, Lacinova L, Flockerzi V, Hofmann F. Structure and functional expression of a new member of the tetrodotoxin-sensitive voltage-activated sodium channel family from human neuroendocrine cells. EMBO J 1995;14:1084-90.

[27] Cestele S, Qu Y, Rogers JC, Rochat H, Scheuer T, Catterall WA. Voltage sensor-trapping: enhanced activation of sodium channels by beta-scorpion toxin bound to the S3-S4 loop in domain II. Neuron 1998;21:919-31.

[28] Wang GK, Wang SY. Veratridine block of rat skeletal muscle Nav1.4 sodium channels in the inner vestibule. J Physiol 2003;548:667-75.

[29] Vickery RG, Amagasu SM, Chang R, Mai N, Kaufman E, Martin J, et al. Comparison of the pharmacological properties of rat Na(V)1.8 with rat Na(V)1.2a and human Na(V)1.5 voltage-gated sodium channel subtypes using a membrane potential sensitive dye and FLIPR. Receptors Channels 2004;10:11-23.

[30] Ulbricht W. Effects of veratridine on sodium currents and fluxes. Rev Physiol Biochem Pharmacol 1998;133:1-54.

[31] Catterall WA, Coppersmith J. Pharmacological properties of sodium channels in cultured rat heart cells. Mol Pharmacol 1981;20:533-42.

[32] Couraud F, Martin-Moutot N, Koulakoff A, Berwald-Netter Y. Neurotoxin-sensitive sodium channels in neurons developing in vivo and in vitro. J Neurosci 1986;6:192-8.

[33] Cusdin FS, Nietlispach D, Maman J, Dale TJ, Powell AJ, Clare JJ, et al. The sodium channel {beta}3-subunit induces multiphasic gating in NaV1.3 and affects fast inactivation via distinct intracellular regions. J Biol Chem 285:33404-12.

[34] Bhattacharya A, Wang Q, Wu N, Wickenden AD. Assay dependent activity of the sodium channel gating modifier protoxin-I: implications for sodium channel drug discovery. FASEB J 2009;23 998.31

[35] Sonnier H, Kolomytkin OV, Marino AA. Resting potential of excitable neuroblastoma cells in weak magnetic fields. Cell Mol Life Sci 2000;57:514-20.

[36] Desai A, Kisaalita WS, Keith C, Wu ZZ. Human neuroblastoma (SH-SY5Y) cell culture and differentiation in 3-D collagen hydrogels for cell-based biosensing. Biosens Bioelectron 2006;21:1483-92.

Statement of conflicts of interest

The authors declare no conflict of interest. The authors declare that they have lodged a patent application relating to high-throughput Na_v assays using the methods described in this paper.

Figures and Legends

Table 1. Primer pairs used for PCR of Na_v subtypes and β subunits. Human Na_v primers were designed using Primer BLAST, and human β subunit primers were as previously described in the literature [11]. For each Na_v subtype and β subunit, GenBank accession numbers, forward and reverse primer sequences, expected PCR product size and locations are listed.

Fig 1. SH-SY5Y cells endogenously express Na_v and accessory β subunits.

Expression of Na_v α and accessory β subunits was assessed by semi-quantitative PCR. (**A**) Amplification of endogenously expressed human $Na_v1.2$, $Na_v1.3$, $Na_v1.4$, $Na_v1.5$ and $Na_v1.7$ was detected in SH-SY5Y cells, with $Na_v1.7$ being the most abundantly expressed Na_v isoforms. (**B**) SH-SY5Y cells endogenously expressed human β2 and β3, but not β1 or β4 subunits. **(C)** Representative gel of Na_v 1.1–$Na_v1.9$ subunits endogenously expressed in SH-SY5Y cells. Far left and right lanes; size marker (bp) **(D)** Representative gel of β1–β4 subunits endogenously expressed in SH-SY5Y cells. Far left lane; size marker (bp). Data are presented as mean ± SEM of n = 3 independent experiments.

Fig 2. Endogenously expressed Na_v channels in SH-SY5Y cells are located at the plasma membrane.

(**A**) and (**B**) SH-SY5Y cells stained with an anti-$Na_v1.7$ antibody show fluorescence located predominantly at the plasma membrane, indicative of functional Na_v expression. Scale bar; 10 μm.

Fig 3. Endogenously expressed Na_v channels in SH-SY5Y cells are functional and TTX-sensitive.

[A-D] Whole-cell patch clamp recordings from SH-SY5Y cells. Na^+ currents were evoked by stepping from -90 mV to 0 mV for 10 ms. (**A**) Concentration-effect of TTX in a single cell. (**B**) Time plot of peak amplitudes of I_{Na} in the presence of increasing concentrations of TTX in a single cell (concentrations indicated by bars). (**C**) Concentration-effect curve of TTX inhibition in SH-SY5Y cells (n = 20). TTX blocked I_{Na} with an IC_{50} of 4.9 nM (pIC_{50} 8.3 ± 0.08) **(D)** Veratridine-elicited tail currents are TTX-sensitive. Veratridine-induced tail currents were evoked by repeating –90 mV to 0 mV step depolarizations five times over a 2.5 second period, at 30 second intervals in the presence of 50 μM veratridine. A prolonged veratridine-induced tail current is rapidly inhibited by TTX (1 μM, within 1.5 min of TTX superfusion; time response plot not shown). (**E**) and (**F**) The Na_v activator veratridine caused a concentration-dependent change in membrane potential with an EC_{50} of 28.5 μM (pEC_{50} 4.54 ± 0.06) that is mediated through activation of TTX-sensitive Na_v as TTX (300 nM) completely blocked responses. (**F**) Addition of veratridine (50 μM) causes a transient change in membrane potential in SH-SY5Y cells mediated through endogenously expressed TTX-sensitive Na_v. Data are presented as mean ± SEM of n = 3–4 wells and are representative of at least 3 independent experiments.

Fig 4. Pharmacological characterization of Ca^{2+} responses elicited by veratridine in SH-SY5Y cells

[A-B] Activation of endogenously expressed TTX-sensitive Na_v by veratridine elicits Ca^{2+} responses in SH-SY5Y cells. (**A**) Veratridine elicited concentration-dependent increases in intracellular Ca^{2+}in SH-SY5Y cells with an EC_{50} of 12.7 μM (pEC_{50} 4.89 ± 0.10, n=11 independent experiments). The Ca^{2+} responses elicited by veratridine were completely blocked in the presence of TTX (300 nM), providing evidence that the responses were mediated solely through TTX-sensitive Na_v isoforms endogenously expressed in SH-SY5Y cells. (**B**) TTX concentration-dependently blocked Ca^{2+} responses elicited by addition of veratridine (50 μM) with an IC_{50} of 8.6 nM; consistent with the inhibition of TTX-sensitive Na_v activated by veratridine. **[C-D]** L-type and N-type VGCC contribute to the veratridine-induced Ca^{2+}response in SH-SY5Y cells. (**C**) The L-type VGCC blocker nifedipine concentration-dependently inhibited veratridine-induced responses by 68-88 % (76 ± 4.4 %) with an IC_{50} of 10.7 nM (pIC_{50} 7.97 ± 0.2). In contrast, the P/Q-type VGCC blocker agatoxin did not significantly inhibit veratridine-elicited Ca^{2+} responses. (**D**) The N-type VGCC blocker CVID concentration-dependently inhibited the veratridine-induced Ca^{2+} responses by 23-33 % (31.8 ± 1.1 %) with an IC_{50} of 19.7 nM (pIC_{50} 7.7 ± 0.5). Block by CVID together with nifedipine was additive, with responses to veratridine completely abolished in the presence of nifedipine (10 μM) and CVID (1 μM) (open square). **[E-F]** Veratridine-induced Ca^{2+} responses are partially mediated by activation of endogenously expressed $Na_v1.2$. (**E**) The $Na_v1.2$/$Na_v1.4$-selective blocker TIIIA reduced veratridine-induced responses with an IC_{50} of 290 nM (pIC_{50} 6.54 ± 0.09). This effect was mediated by $Na_v1.2$, as the $Na_v1.4$-selective blocker GIIIA did not affect veratridine responses at concentrations up to 10 μM. (**F**) In the presence of TIIIA (1 μM), the magnitude of

the veratridine-induced responses was decreased to 58.7 ± 2.8 % of maximum and there was a small but significant ($p< 0.05$) rightward shift of the veratridine concentration-response curve to an EC_{50} of 45.8 μM (pEC_{50} 4.33 ± 0.16). **[G-H]** Activation of $Na_v1.7$ contributes to the veratridine-induced Ca^{2+} response in SH-SY5Y cells. **(G)** In the presence of TIIIA (1 μM), the $Na_v1.7$-selective blocker ProTxII concentration-dependently inhibited veratridine-induced responses with an IC_{50} of 206.9 pM (pIC_{50} 9.68 ± 0.15), consistent with inhibition of $Na_v1.7$. In the absence of TIIIA, ProTxII concentration-dependently inhibited veratridine-induced responses with a two-site fit with IC_{50}s of 151.7 pM and 56 nM (pIC_{50} 9.82 ± 0.23 and pIC_{50} 7.25 ± 0.26), respectively. (**H**) Activation of endogenously expressed $Na_v1.2$ and $Na_v1.7$ by veratridine (50 μM) results in an assay with excellent performance, with *Z'* scores of 0.7 ± 0.05. Data are presented as mean ± SEM of n = 3-4 wells and are representative of at least 3 independent experiments.

Fig 5. ProTxII and TIIIA inhibit endogenously expressed TTX-sensitive Na_v in SH-SY5Y cells.

Na^+ currents were evoked by stepping from –90 mV to 0 mV for 10 ms. ProTxII (30 nM) or TIIIA (1 μM) were initially examined independently of each other, before examining their combined inhibitory effects of I_{Na}. (**A**) An illustration showing the progressive inhibition of I_{Na} by superfusion of ProTxII (30 nM), TIIIA (1 μM) and TTX (1 μM) in a single SH-SY5Y cell. (**B**) Time plot of a single SH-SY5Y cell showing effects of first ProTxII (30 nM), then ProTxII (30 nM) and TIIIA (1 μM) superfusion. TTX (1 μM) was superfused onto the cell at the end of the experiment to inhibit any remaining Na_v. Bars indicate the duration of antagonist superfusion. (**C**) ProTxII (30 nM) and TIIIA (1 μM) both significantly inhibit I_{Na} ($p < 0.0001$). In

two cells, combined application of ProTxII and TIIIA produced greater inhibition of I_{Na} than either alone. Numbers in brackets above column bars indicate the number of cells examined for each antagonist. (**D)** Veratridine-induced tail currents of endogenously expressed TTX-sensitive Na_v in SH-SY5Y cells can be inhibited by ProTxII and TIIIA. Veratridine-induced tail currents were evoked by repeating -90 mV to 0 mV step depolarizations five times over a 2.5 second period, at 30 second intervals in the presence of veratridine (50 μM). TIIIA (1 μM) or ProTxII (30 nM) both significantly ($p < 0.001$) inhibited veratridine-induced tail currents. Combined application of ProTxII and TIIIA produced significantly ($p < 0.001$) greater inhibition of the veratridine-induced tail current than either alone. Numbers in brackets above column bars represent the number of cells per respective experiment.

Fig 6. The $Na_v1.7$-selective agonist OD1 potentiates veratridine-induced Ca^{2+} responses.

Increases in intracellular Ca^{2+} were measured in Fluo-4-loaded SH-SY5Y cells using the FLIPR^{TETRA+} plate reader. **(A)** Treatment with increasing concentrations of OD1 (1-30 nM) shifted the veratridine concentration-response curve to the left, without affecting maximal Ca^{2+} responses. Dotted line indicates OD1-potentiated Ca^{2+} responses in the presence of 2 μM veratridine. **(B)** OD1 concentration-dependently potentiated Ca^{2+} responses induced by veratridine (2 μM) with an EC_{50} of 3.0 nM (pEC_{50} 8.52 ± 0.01, n=3 independent experiments). **(C)** The $Na_v1.7$-specific antagonist ProTxII concentration-dependently inhibited Ca^{2+} responses elicited by OD1 (30 nM) and veratridine (2 μM) with an IC_{50} of 1.3 nM (pIC_{50} 8.88 ± 0.14, n=3 independent experiments). Data are presented as mean ± SEM of n = 3-8 wells and are representative of at least 2 independent experiments.

Fig 7. Veratridine-induced Ca^{2+} responses in SH-SY5Y cells are amenable to pharmacological characterisation of small molecule Na_v inhibitors. Vertatridine-induced Ca^{2+} responses in SH-SY5Y cells are concentration-dependently inhibited by clinically used small molecule Na_v inhibitors, with IC_{50} values in accordance with literature values.

Figure 1

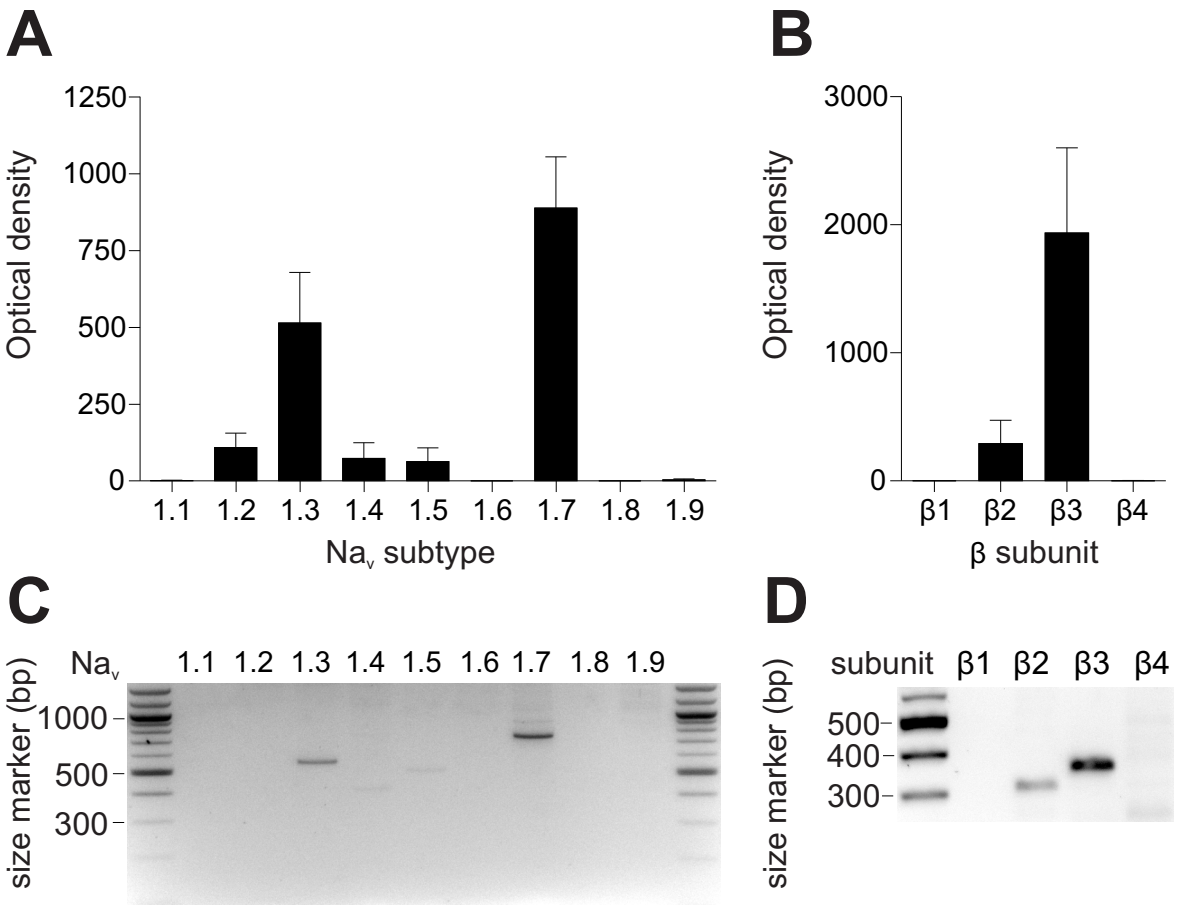
A
Optical density
1250
1000
750
500
250
0
1.1 1.2 1.3 1.4 1.5 1.6 1.7 1.8 1.9
Na$_v$ subtype
B
Optical density
3000
2000
1000
0
β1 β2 β3 β4
β subunit
C
Na$_v$ 1.1 1.2 1.3 1.4 1.5 1.6 1.7 1.8 1.9
size marker (bp)
1000
500
300
D
subunit β1 β2 β3 β4
size marker (bp)
500
400
300

Figure 2

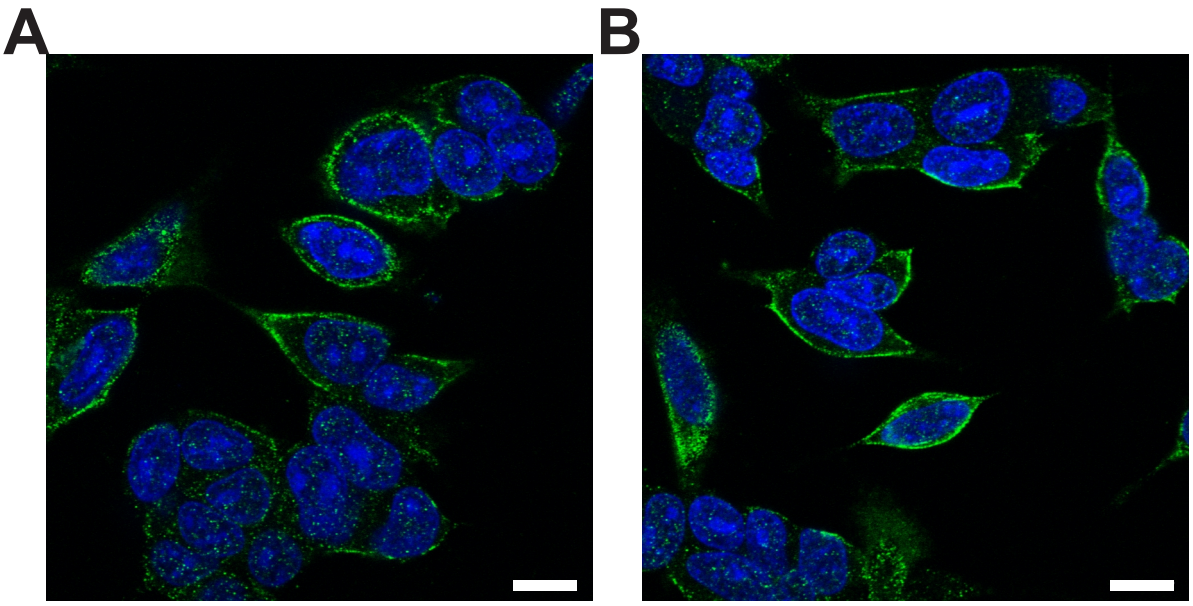

Figure 3

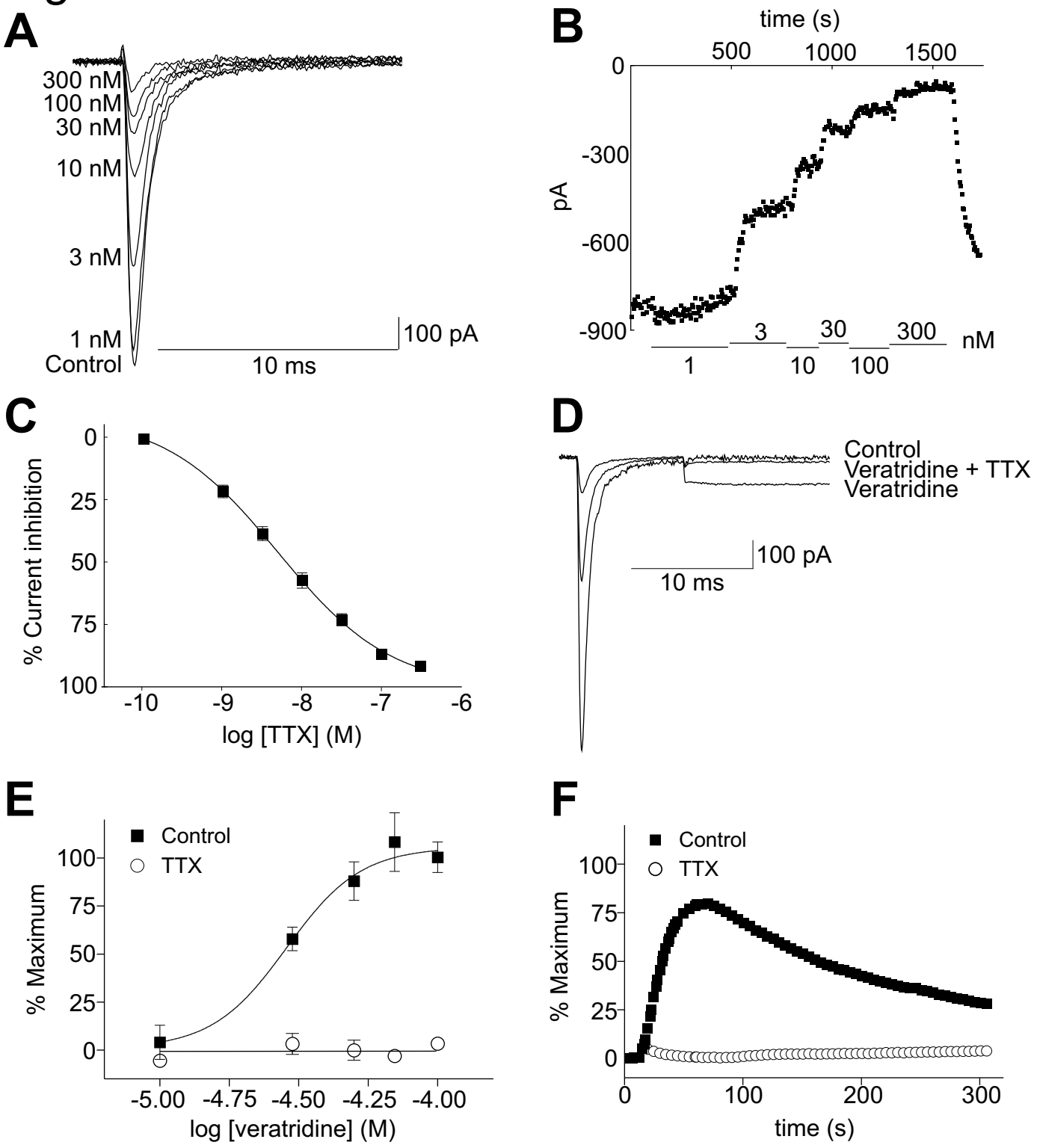
A
300 nM
100 nM
30 nM
10 nM
3 nM
1 nM
Control
100 pA
10 ms
B
time (s)
500
1000
1500
0
-300
-600
-900
pA
1
3
10
30
100
300
nM
C
% Current inhibition
0
25
50
75
100
-10
-9
-8
-7
-6
log [TTX] (M)
D
Control
Veratridine + TTX
Veratridine
100 pA
10 ms
E
Control
TTX
% Maximum
100
75
50
25
0
-5.00
-4.75
-4.50
-4.25
-4.00
log [veratridine] (M)
F
Control
TTX
% Maximum
100
75
50
25
0
0
100
200
300
time (s)

Figure 4

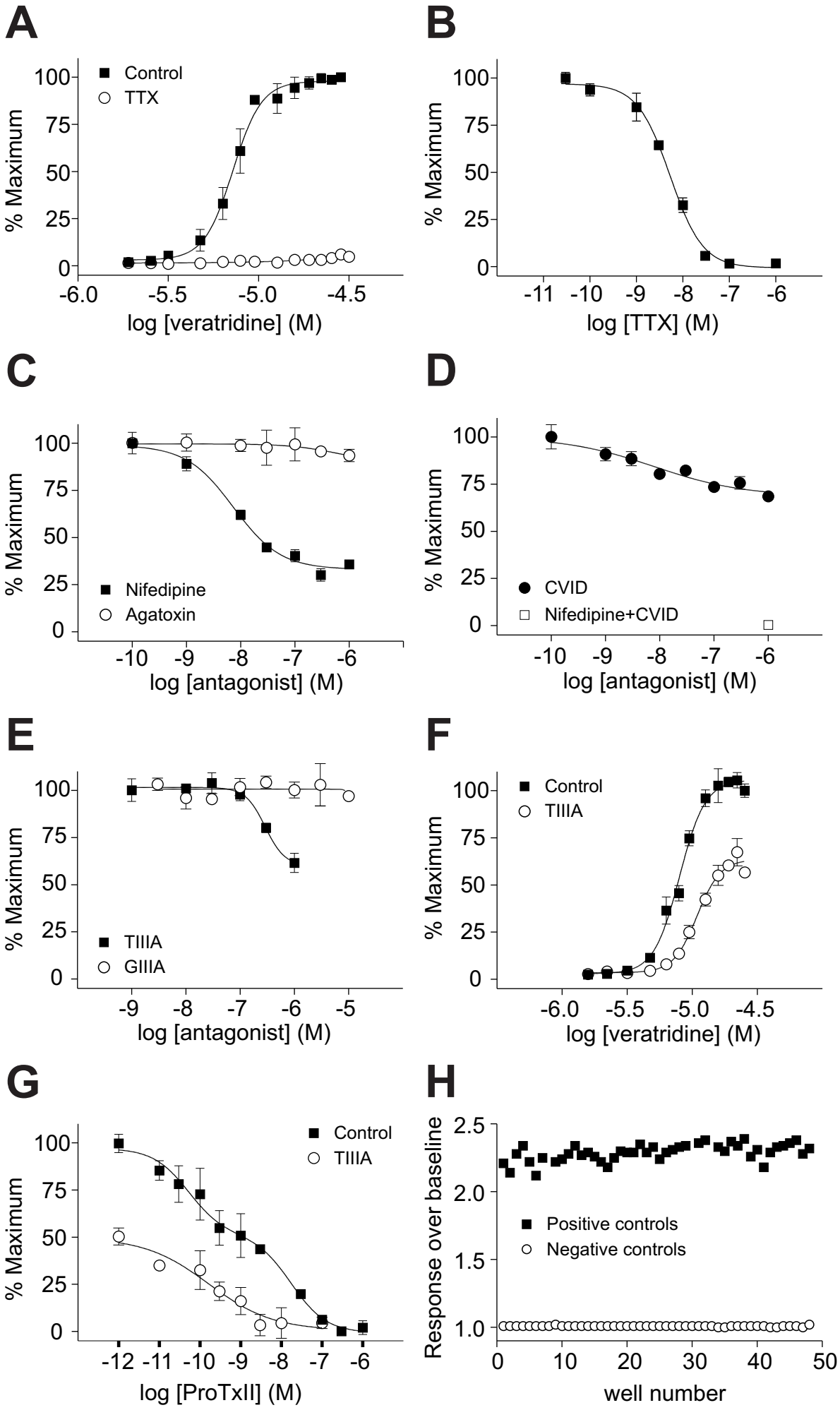
A
Control
TTX
% Maximum
log [veratridine] (M)
B
% Maximum
log [TTX] (M)
C
Nifedipine
Agatoxin
% Maximum
log [antagonist] (M)
D
CVID
Nifedipine+CVID
% Maximum
log [antagonist] (M)
E
TIIIA
GIIIA
% Maximum
log [antagonist] (M)
F
Control
TIIIA
% Maximum
log [veratridine] (M)
G
Control
TIIIA
% Maximum
log [ProTxII] (M)
H
Positive controls
Negative controls
Response over baseline
well number

Figure 5

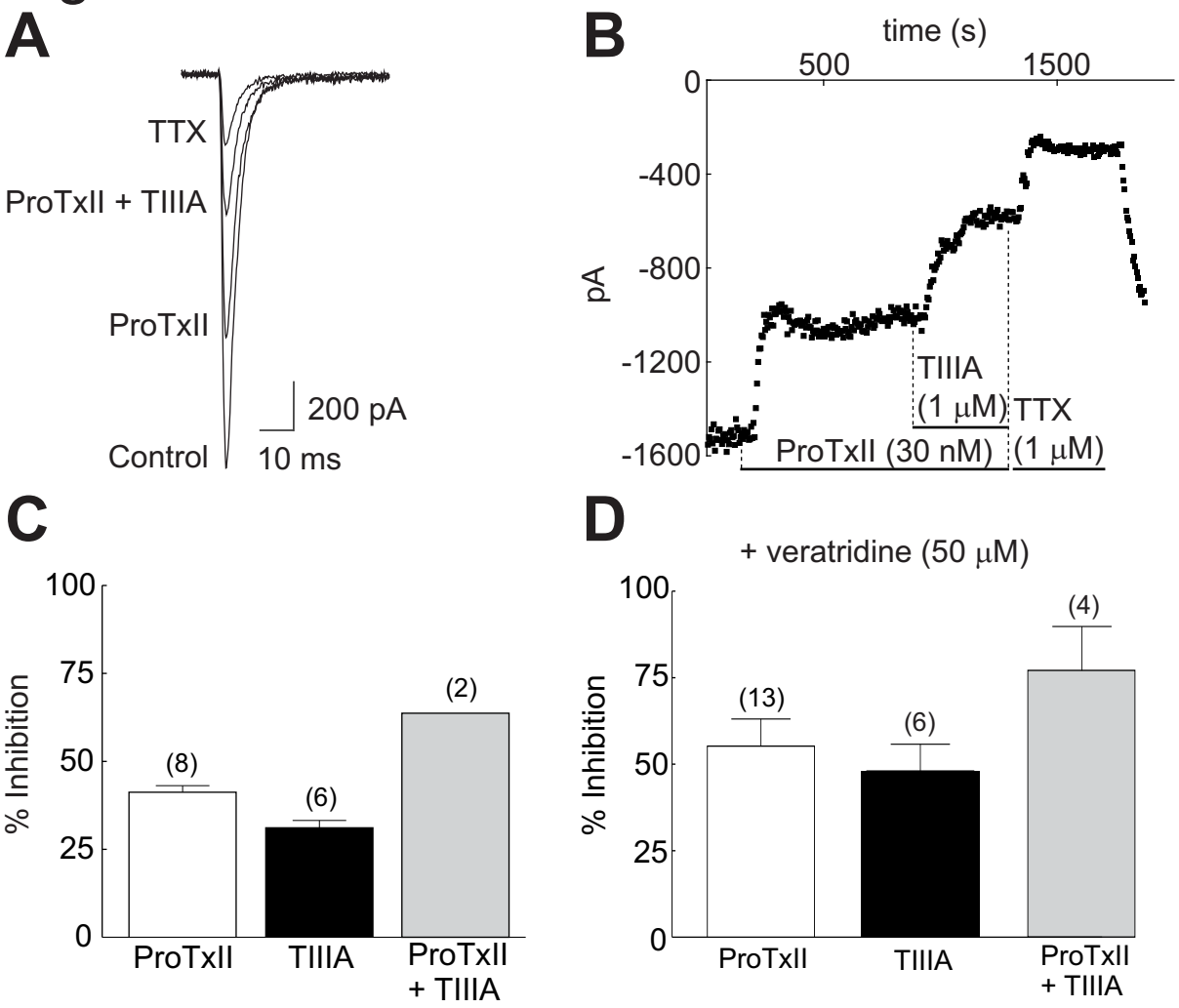
A
TTX
ProTxII + TIIIA
ProTxII
200 pA
Control
10 ms
B
time (s)
500
1500
0
-400
-800
-1200
-1600
pA
TIIIA
(1 μM)
TTX
(1 μM)
ProTxII (30 nM)
C
100
75
50
25
0
% Inhibition
(8)
(6)
(2)
ProTxII
TIIIA
ProTxII
+ TIIIA
D
+ veratridine (50 μM)
100
75
50
25
0
% Inhibition
(13)
(6)
(4)
ProTxII
TIIIA
ProTxII
+ TIIIA

Figure 6

A

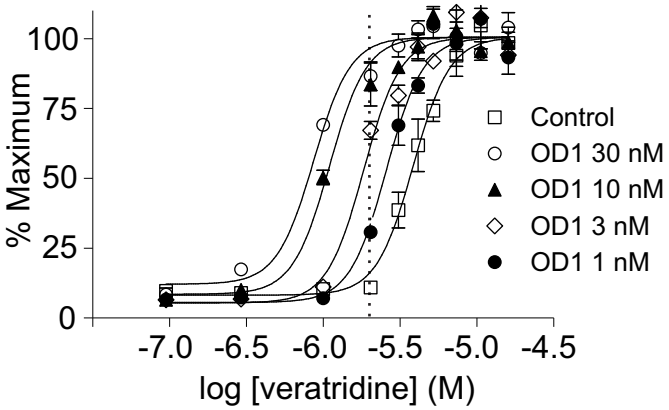
100
75
50
25
0
% Maximum
-7.0
-6.5
-6.0
-5.5
-5.0
-4.5
log [veratridine] (M)
Control
OD1 30 nM
OD1 10 nM
OD1 3 nM
OD1 1 nM

B

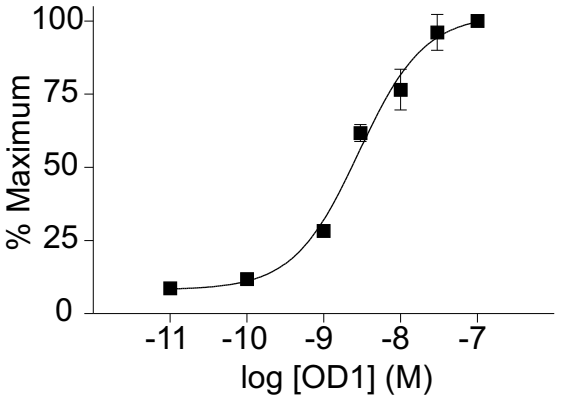
100
75
50
25
0
% Maximum
-11
-10
-9
-8
-7
log [OD1] (M)

C

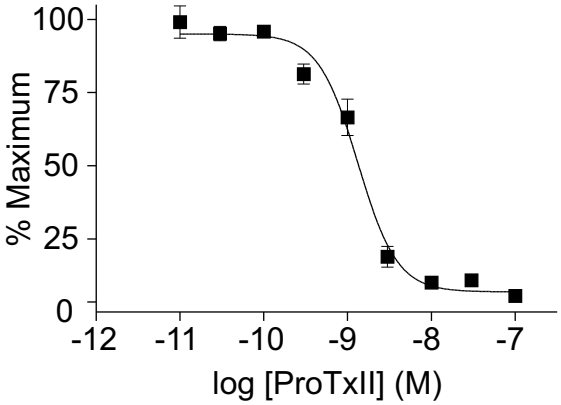
100
75
50
25
0
% Maximum
-12
-11
-10
-9
-8
-7
log [ProTxII] (M)

Figure 7

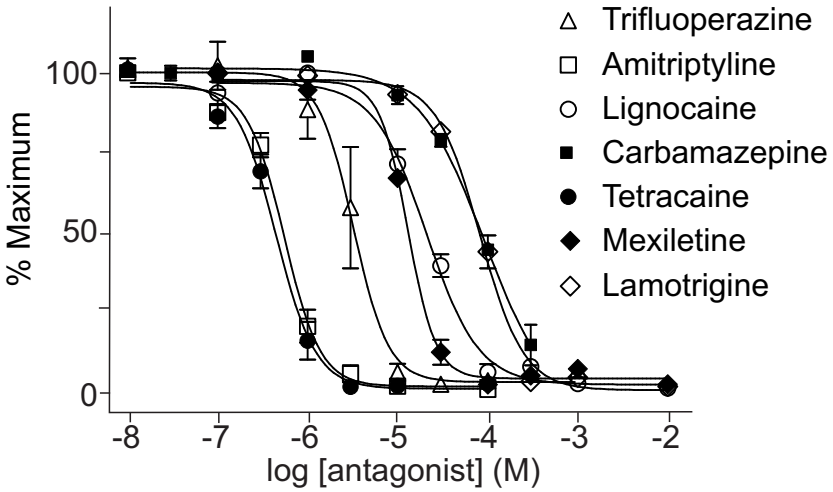
Trifluoperazine
Amitriptyline
Lignocaine
Carbamazepine
Tetracaine
Mexiletine
Lamotrigine
% Maximum
100
50
0
-8
-7
-6
-5
-4
-3
-2
log [antagonist] (M)